ICTP, Trieste, 25 July 2022

# Impact of tropical ocean SSTs on the late winter signal over the North Atlantic-European region

Sara Ivasić (sara.ivasic@gfz.hr), Ivana Herceg Bulić and Margareta Popović

University of Zagreb, Faculty of Science, Department of Geophysics

## North Atlantic-European (NAE) region

- under the dominant influence of the North Atlantic Oscillation (NAO)
- large internal variability of the atmosphere → affects seasonal predictability

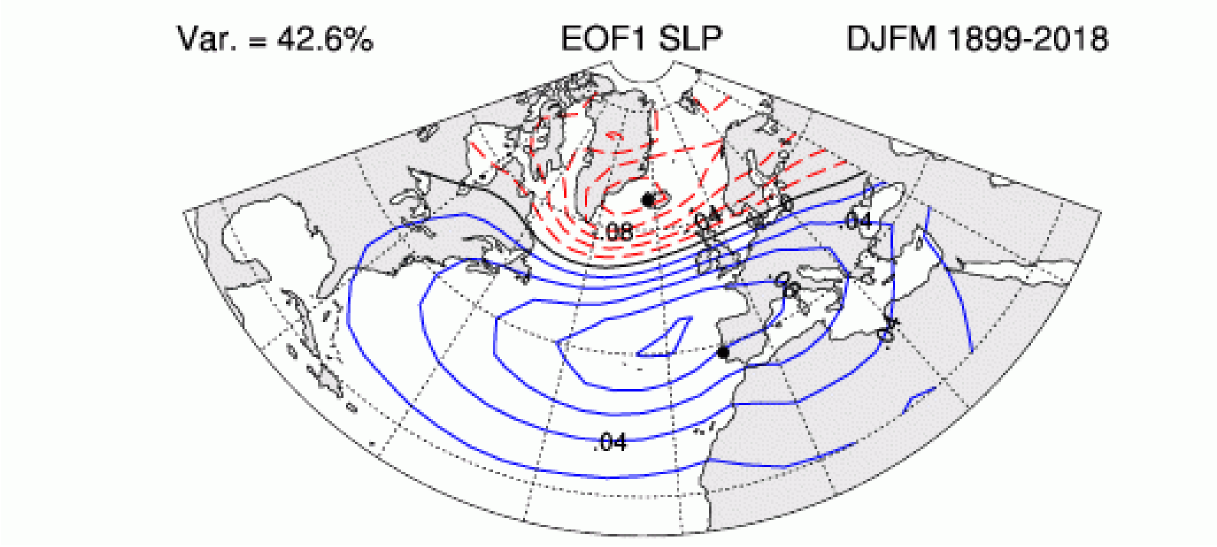


https://climatedataguide.ucar.edu/climate-data/hurrell-north-atlantic-oscillation-nao-index-station-based

## North Atlantic-European (NAE) region

- under the dominant influence of the North Atlantic Oscillation (NAO)
- large internal variability of the atmosphere → affects seasonal predictability

➢ idea: improve seasonal predictability by using strong sources of signal outside the region of interest

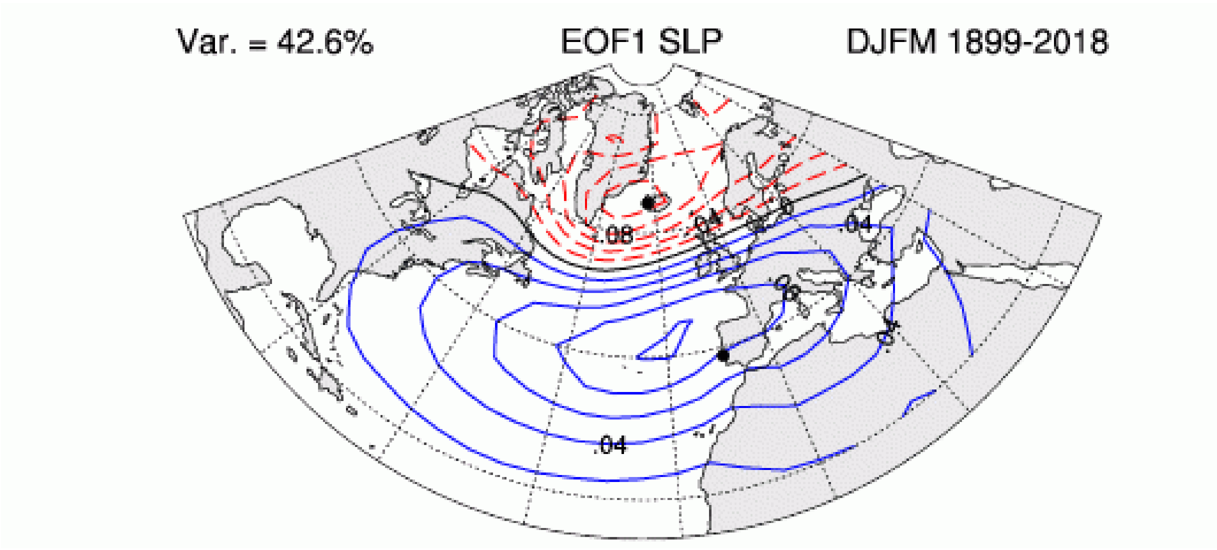


https://climatedataguide.ucar.edu/climate-data/hurrell-north-atlantic-oscillation-nao-index-station-based

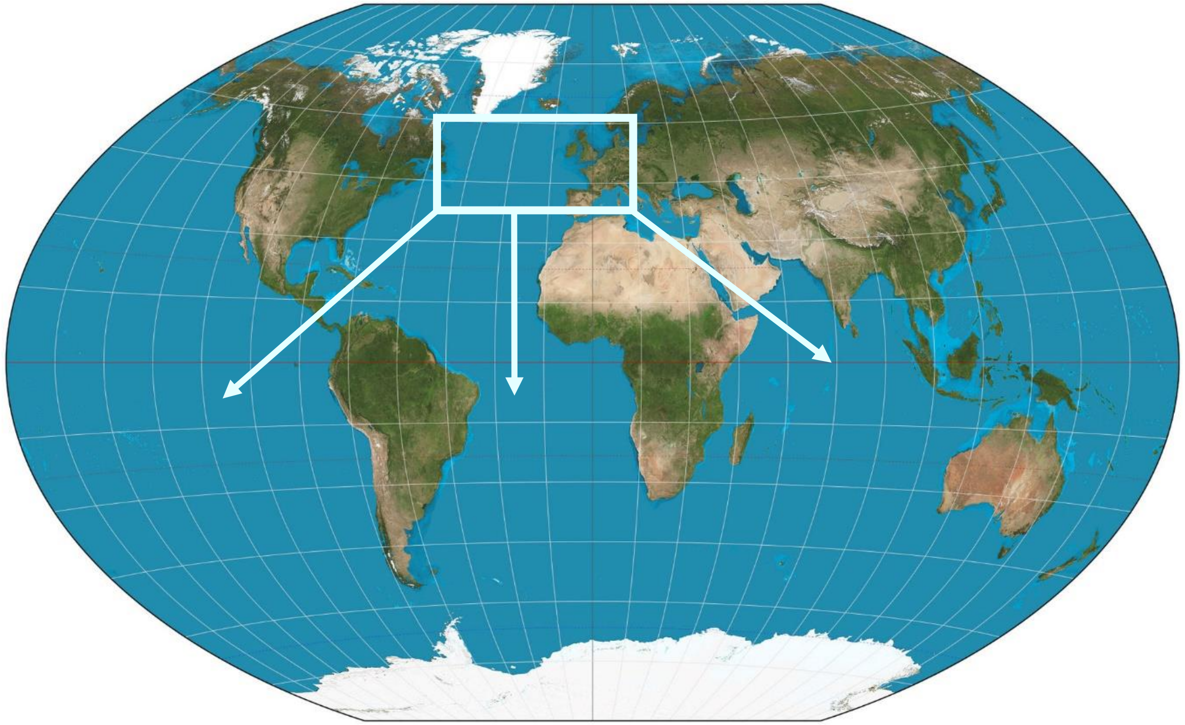

# El Niño-Southern Oscillation (ENSO)

- quasiperiodic phenomenon in the atmosphere-ocean system
- global impacts on climate variability
- affects remote regions through teleconnections

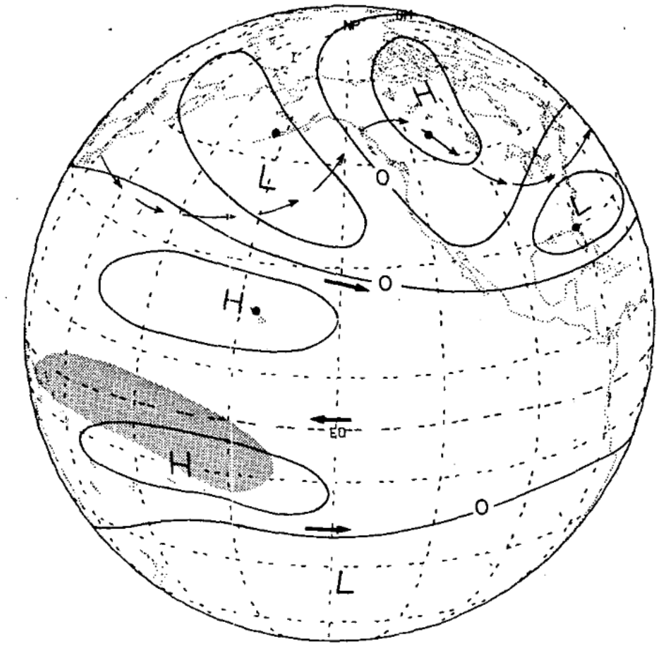

Horel and Wallace (1981)

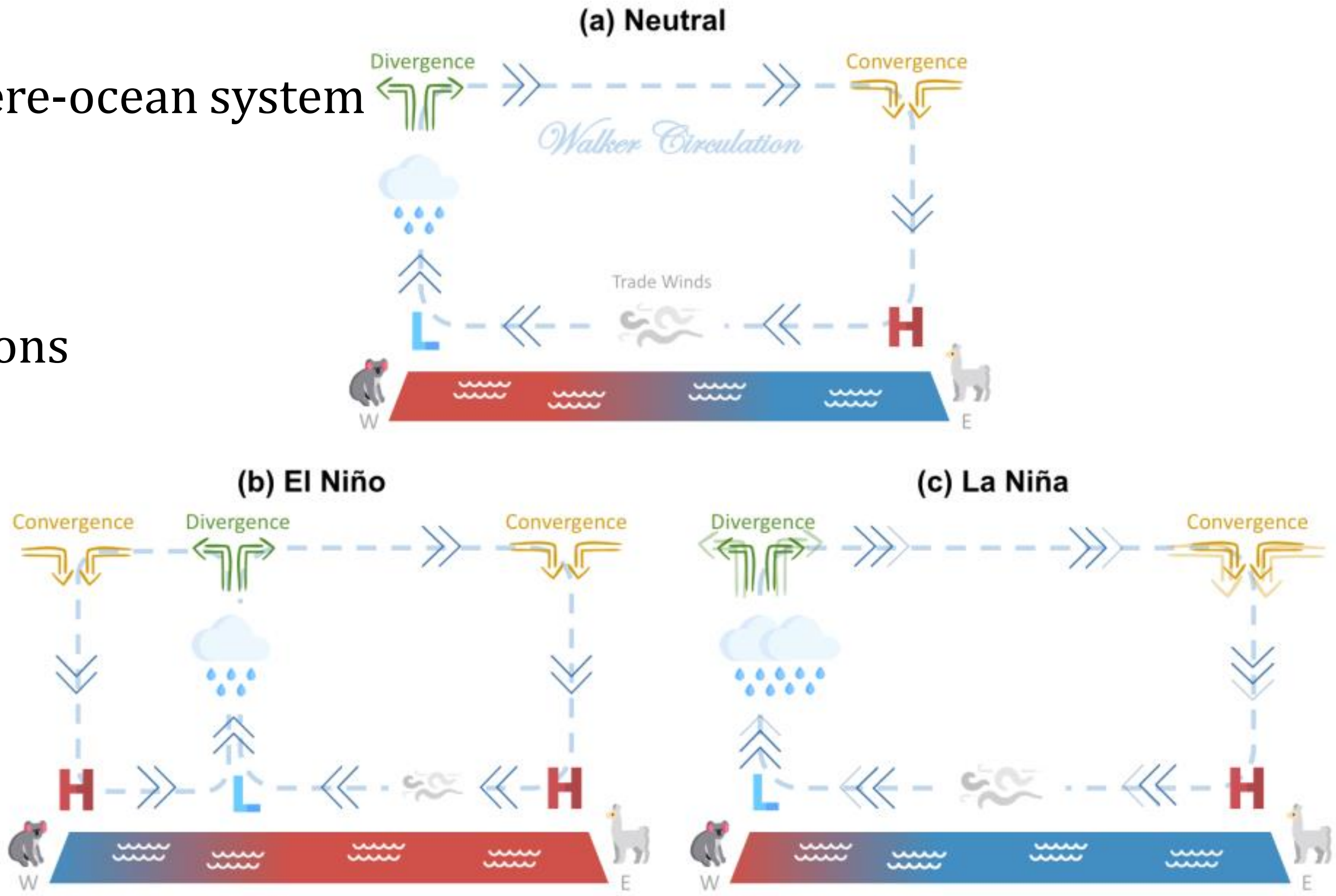


Mezzina, B 2022, *Dynamics of the late-winter ENSO teleconnection to the North Atlantic-European region*, PhD thesis, University of Barcelona, Barcelona, http://hdl.handle.net/2445/182562

- goal → distinguish internal from boundary-forced variability
- ensembles of numerical simulations used to estimate signal and noise

**ICTP AGCM** (SPEEDY; T30-L8)

- intermediately complex AGCM → computationaly inexpensive
- parametrizations: SW and LW radiation, large-scale condensation, convection, surface fluxes of momentum, heat and moisture, and vetical diffusion
- successful in simulating the main features of ENSO-related global teleconnections (Abid et al. 2000; Herceg-Bulić et al. 2012, 2017; Kucharski et al. 2006, 2013)

## ICTP AGCM experiments

- six ensembles of numerical simulations
- monthly varying NOAA ERSST V3 SST anomalies set as lower-boundary forcing only in limited ocean areas
- climatological exp → no SST anomalies
- period: 1854-2010
- JFM geopotential height at 200 hPa
- output filtered with a high-pass filter with a cut off period of 11 years

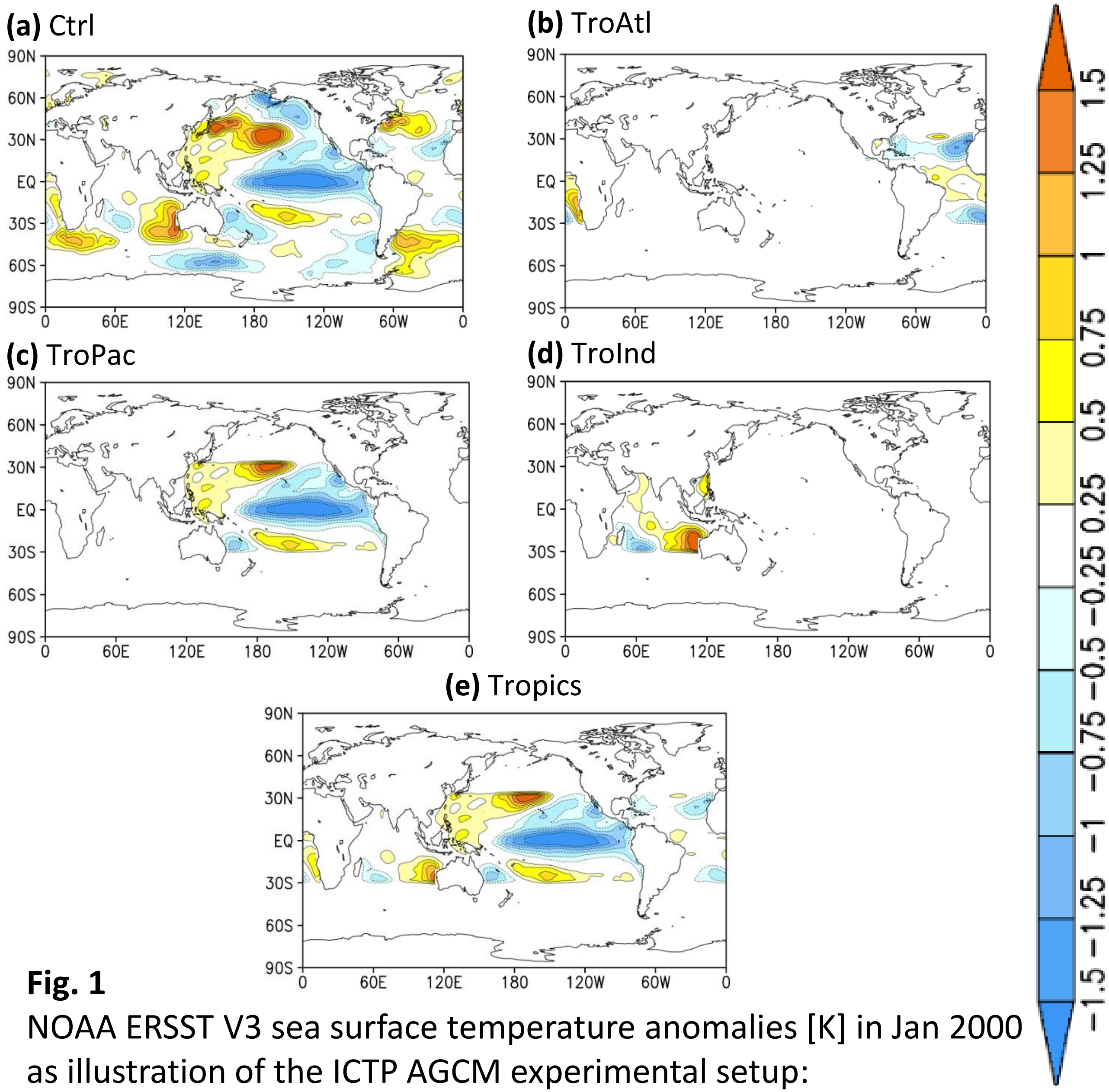


**Fig. 1**
NOAA ERSST V3 sea surface temperature anomalies [K] in Jan 2000 as illustration of the ICTP AGCM experimental setup:
(a) Ctrl, (b) TroAtl, (c) TroPac, (d) TroInd, and (e) Tropics

## Empirical Orthogonal Functions analysis

- linear decomposition tehnique
- result: orthogonal EOF patterns and corresponding time series (PCs) which explain the largest part of variability
- EOFs based on all ensemble members vs. enseble mean

## Signal-to-noise optimal patterns method

- method described in the paper by Straus and Shukla et al. (2003)
- all ensemble members used to find a hierarchy of modes sorted by their signal-to-noise ratio
- result: OPT patterns which have the maximum signal-to-noise ratio
- not suitable for observations

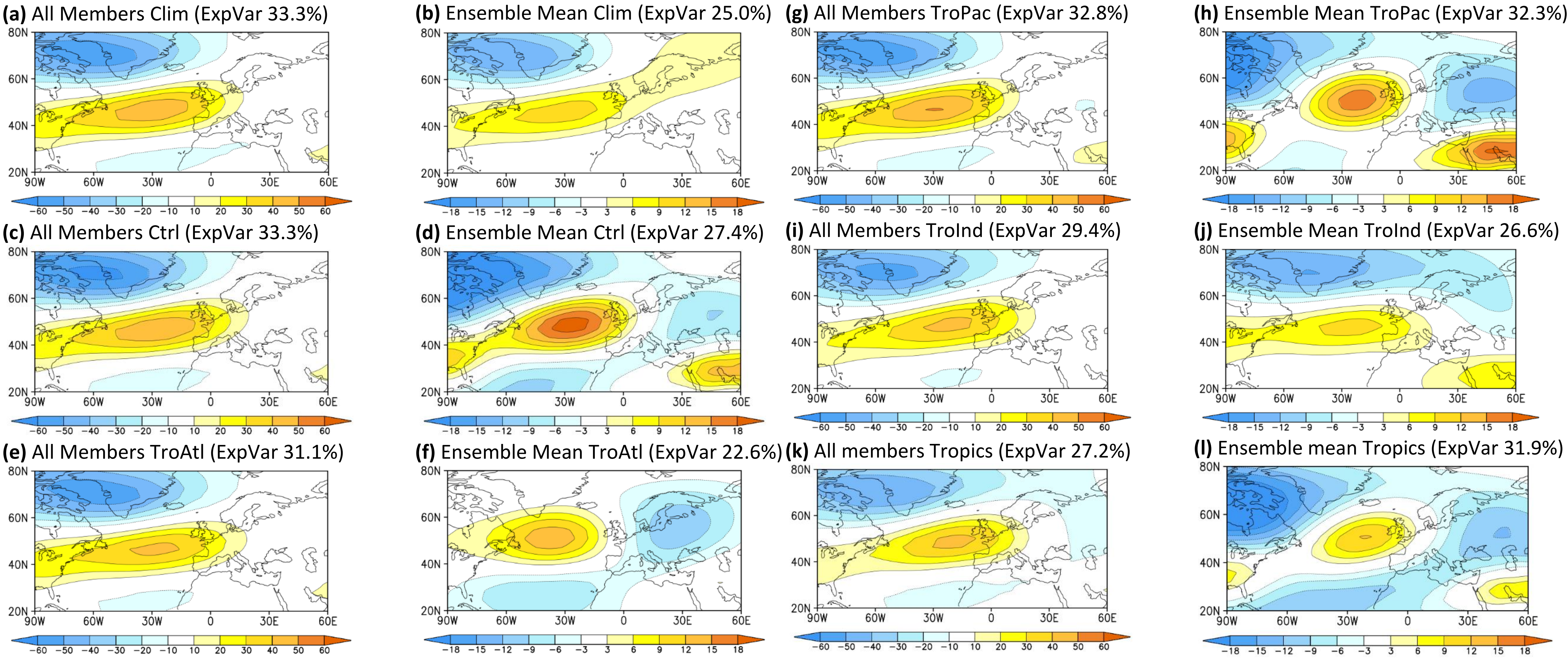


**Fig. 2** EOF1 pattern of JFM geopotential heights at 200 hPa (GH200) [m] based on all ensemble members and based on the ensemble mean in the period 1855-2010 in ICTP AGCM experiments: Clim, Ctrl, TroAtl, TroPac, TroInd, and Tropics. The percentage of explained variance (ExpVar) associated with each of the EOF patterns is indicated by the number in brackets.

Following the definitions from Branković and Molteni (2004):

**Signal estimate**

$$\sigma_s^2 = \frac{1}{N}\sum_{j=1}^{N}\left(\overline{x}_j - \overline{x}\right)^2$$

Ensemble mean in the *j*-th year:

$$\overline{x}_j = \frac{1}{M}\sum_{i=1}^{M} x_{ij}$$

**Noise estimate**

$$\sigma_n^2 = \frac{1}{N}\sum_{j=1}^{N}\left[\frac{1}{M}\sum_{i=1}^{M}\left(x_{ij} - \bar{x}_j\right)^2\right]$$

Climatological mean of the ensemble mean:

$$\overline{x} = \frac{1}{N}\sum_{j=1}^{N}\overline{x}_j$$

N – number of years (156)
M – number of ensemble members (35)

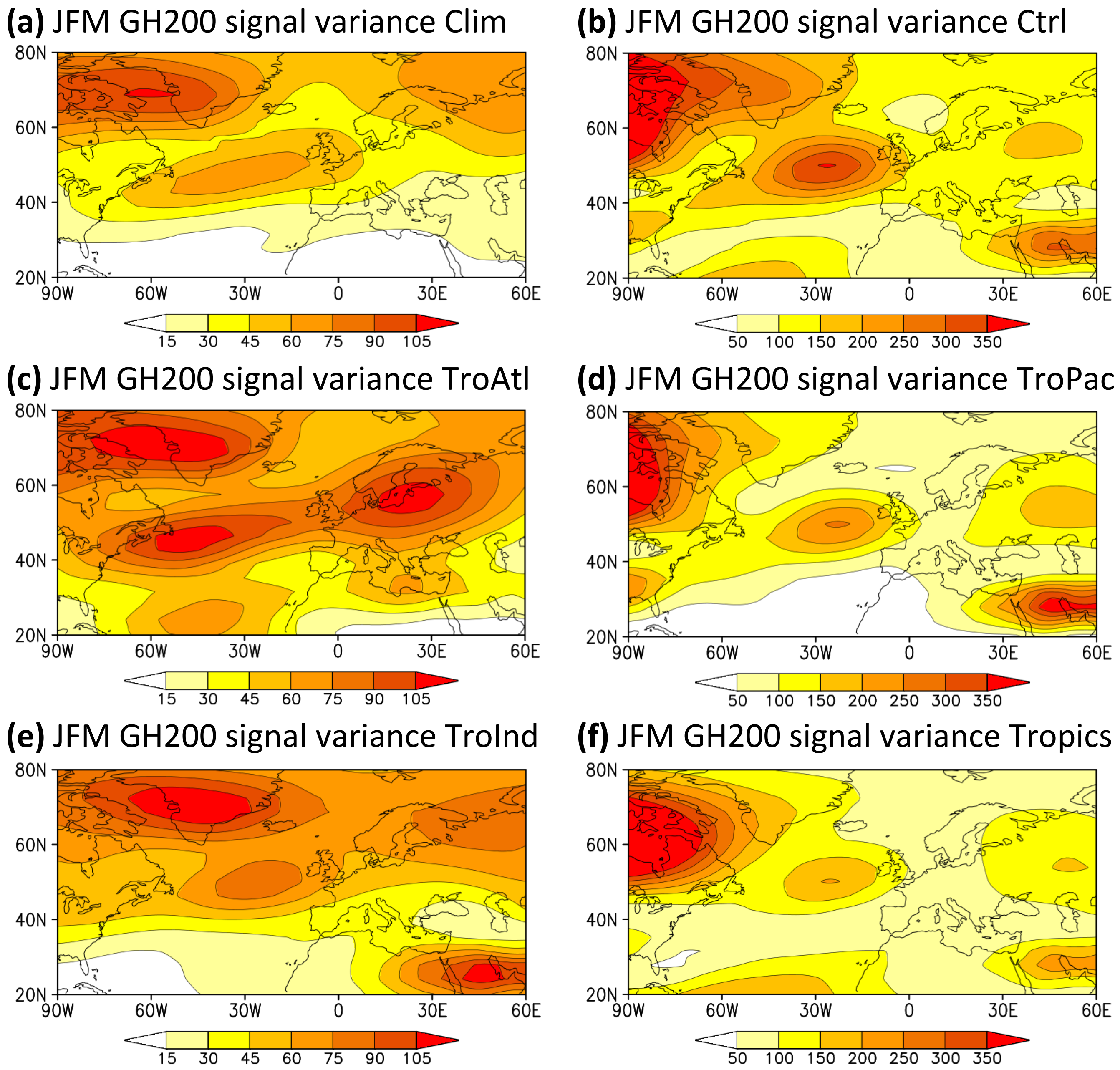


**Fig. 3** JFM signal variance of geopotential heights at 200 hPa (GH200) [m$^2$] in ICTP AGCM experiments

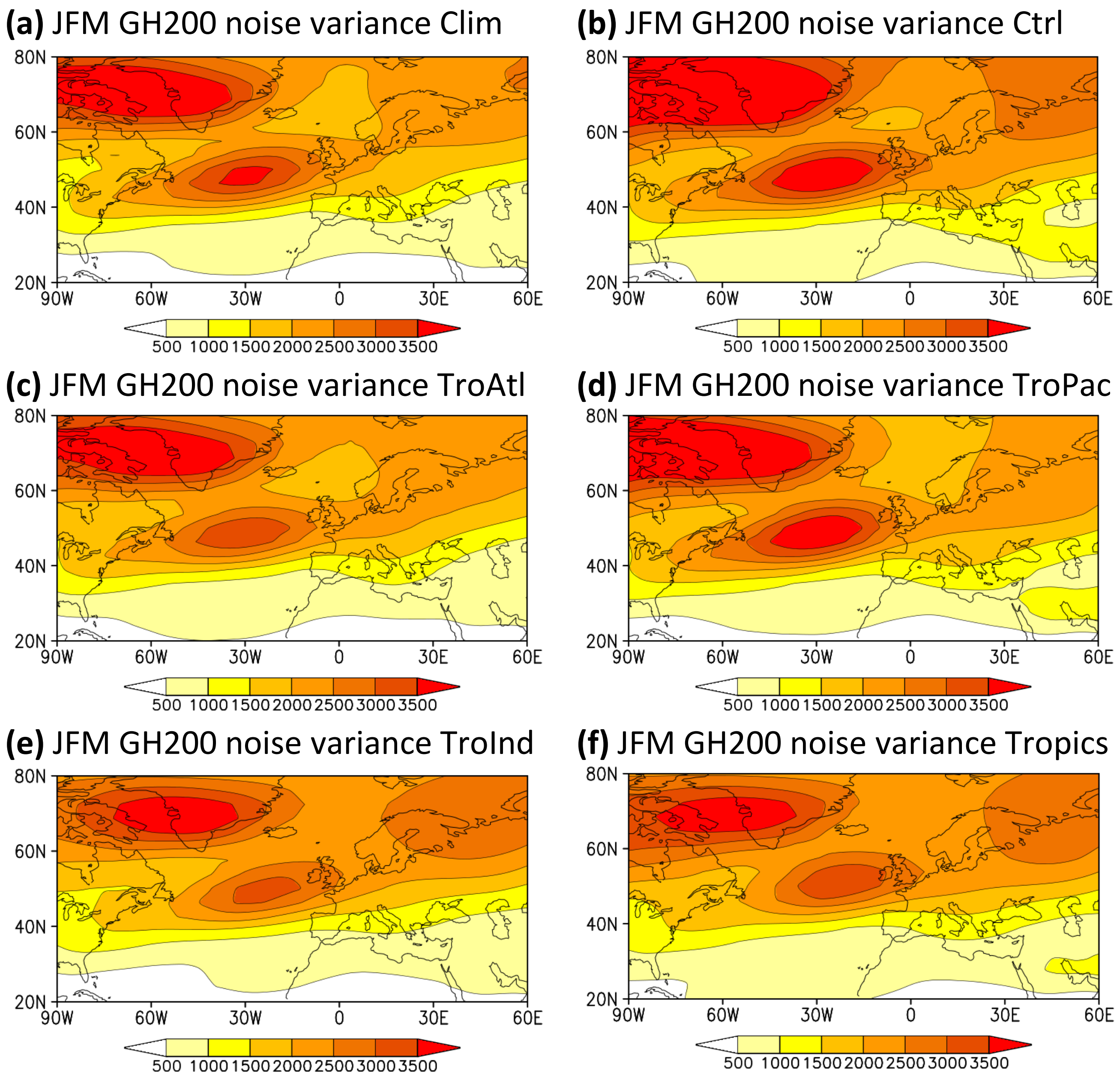


**Fig. 4** JFM noise variance of geopotential heights at 200 hPa (GH200) [$m^2$] in ICTP AGCM experiments

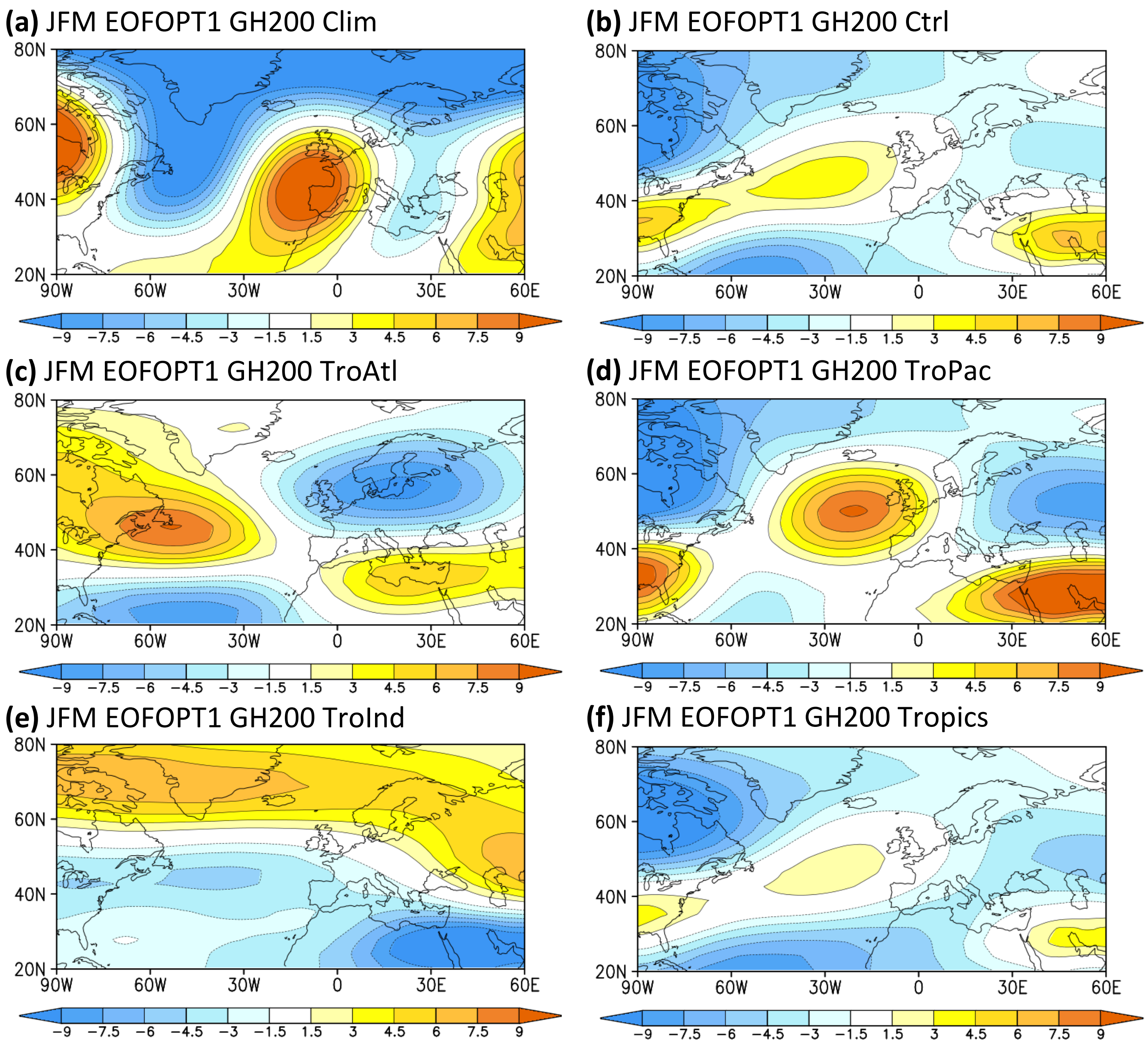


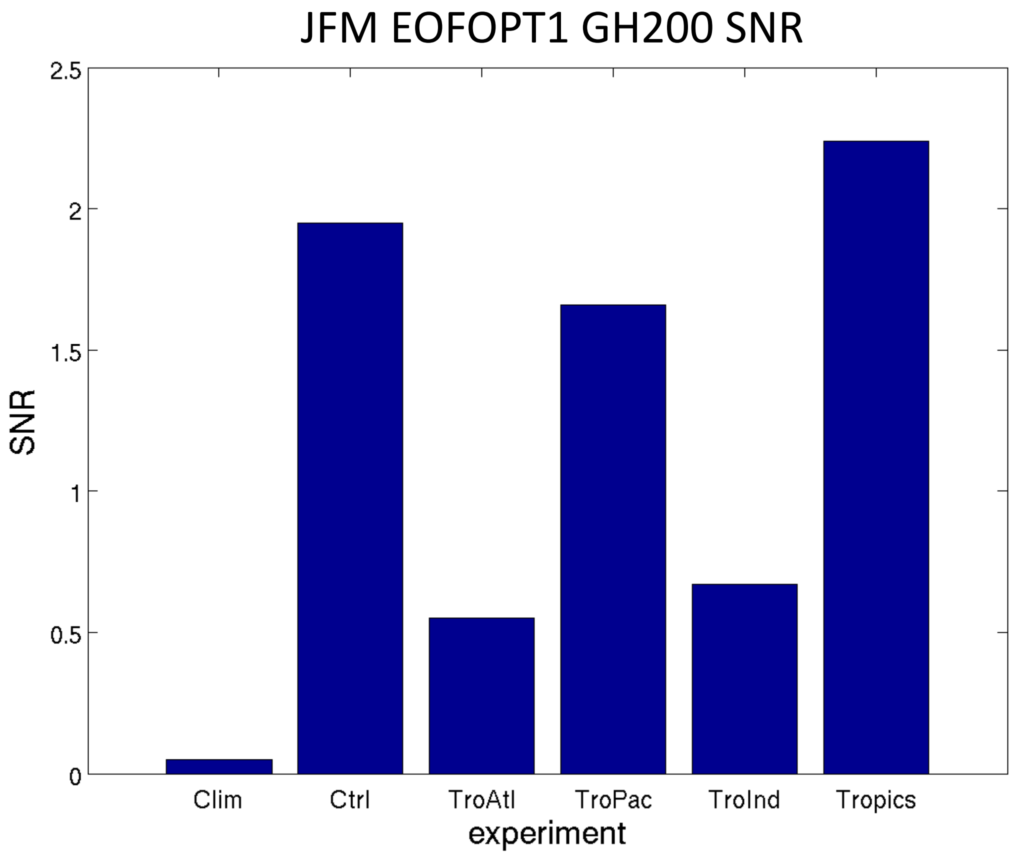


**Fig. 5** First spatial pattern (EOFOPT1) of JFM GH200 [m] in the signal-to-noise optimal patterns method in the period 1855-2010 for ICTP AGCM experiments:(a) Clim, (b) Ctrl, (c) TroAtl, (d) TroInd, (e) TroPac, and (f) Tropics. Panel (g) shows the corresponding signal-to-noise ratio (SNR) of the EOFOPT1 mode. All SNR values are considered statistically significant according to the F-test for the ratio of variances on the 95% confidence level.

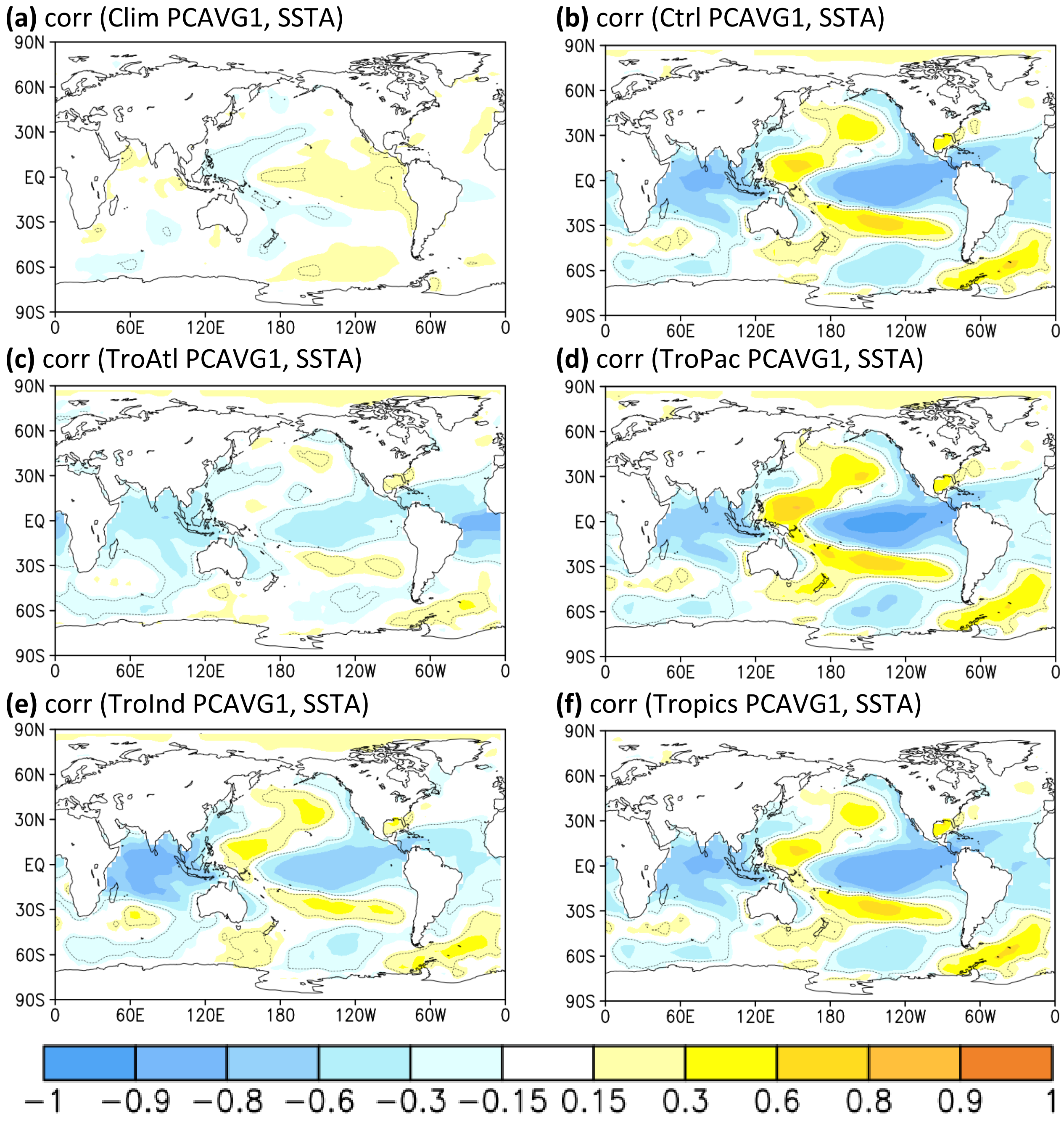


## Correlation of GH200 with observed SSTAs

**Fig. 6** Correlation of global NOAA ERSST V3 SST anomalies and the time series associated with the first optimal pattern (PCAVG1) of JFM GH200 in the period 1855-2010 for ICTP AGCM experiments: (a) Clim, (b) Ctrl, (c) TroAtl, (d) TroPac, (e) TroInd, and (f) Tropics. All statistically significant values based on the two-tailed Student’s t-test on the 95% confidence level are encircled by dashed contours.

The EOF analysis was applied on the observed SST anomalies in the same areas as the SST-boundary forcing within ICTP AGCM experiments.

**Table 1** Correlation between the first principal component (PC1) of NOAA sea surface temperature anomalies (SSTA) and the time series associated with the first optimal pattern (PCAVG1) of geopotential heights at 200 hPa (GH200) in JFM season in ICTP AGCM experiments. All values are statistically significant based on the two-tailed Student's t-test on the 95% confidence level.

| | Ctrl GH200 PCAVG1 | TroAtl GH200 PCAVG1 | TroPac GH200 PCAVG1 | TroInd GH200 PCAVG1 | Tropics GH200 PCAVG1 |
|---|---|---|---|---|---|
| TroAtl SSTA PC1 | **0.81** | **0.42** | **0.77** | **0.47** | **0.81** |
| TroPac SSTA PC1 | **0.88** | **0.34** | **0.95** | **0.60** | **0.87** |
| TroInd SSTA PC1 | **0.81** | **0.51** | **0.71** | **0.86** | **0.78** |
| Tropics SSTA PC1 | **0.91** | **0.41** | **0.95** | **0.66** | **0.90** |

**Table 2** Correlation between the first principal component (PC1) of NOAA sea surface temperature anomalies (SSTA) and PC1 of GH200 in JFM season calculated for the ensemble mean of each ICTP AGCM experiment. All values are statistically significant based on the two-tailed Student's t-test on the 95% confidence level

| | Ctrl GH200 PC1 EnsMean | TroAtl GH200 PC1 EnsMean | TroPac GH200 PC1 EnsMean | TroInd GH200 PC1 EnsMean | Tropics GH200 PC1 EnsMean |
|---|---|---|---|---|---|
| TroAtl SSTA PC1 | **0.55** | **0.33** | **0.69** | **-0.25** | **0.69** |
| TroPac SSTA PC1 | **0.70** | **0.27** | **0.87** | **-0.33** | **0.81** |
| TroInd SSTA PC1 | **0.47** | **0.37** | **0.64** | **-0.52** | **0.59** |
| Tropics SSTA PC1 | **0.69** | **0.31** | **0.86** | **-0.37** | **0.81** |

## ICTP AGCM experiments

- SST boundary forcing, especially in the tropical Pacific, enhances potential predictability of the late-winter atmospheric circulation over the North Atlantic-European region
- boundary-forced signal can be detected in the first EOF based on the ensemble mean and the first optimal pattern, which has the highest signal-to-noise ratio
- time series connected to the optimal pattern is spatially and temporally connected to the variability of the observed SSTs

## ICTP AGCM experiments

- SST boundary forcing, especially in the tropical Pacific, enhances potential predictability of the late-winter atmospheric circulation over the North Atlantic-European region

- boundary-forced signal can be detected in the first EOF based on the ensemble mean and the first optimal pattern, which has the highest signal-to-noise ratio

- time series connected to the optimal pattern is spatially and temporally connected to the variability of the observed SSTs

Results were first published in the paper:

Ivasić, S., & Herceg-Bulić, I. (2022). A modelling study of the impact of tropical SSTs on the variability and predictable components of seasonal atmospheric circulation in the North Atlantic-European region. Climate Dynamics, https://doi.org/10.1007/s00382-022-06357-3

# References


- Abid MA, Kucharski F, Molteni F, et al (2020) Separating the Indian and Pacific Ocean impacts on the Euro-Atlantic response to ENSO and its transition from early to late winter. J Clim 1–57. https://doi.org/10.1175/jcli-d-20-0075.1
- Branković, Č., Molteni, F. Seasonal climate and variability of the ECMWF ERA-40 model. Climate Dynamics 22, 139–155 (2004).
- Herceg-Bulić I, Branković Č, Kucharski F (2012) Winter ENSO teleconnections in a warmer climate. Clim Dyn 38:1593–1613. https://doi.org/10.1007/s00382-010-0987-8
- Herceg-Bulić I, Mezzina B, Kucharski F, et al (2017) Wintertime ENSO influence on late spring European climate: the stratospheric response and the role of North Atlantic SST. Int J Climatol 37:87–108. https://doi.org/10.1002/joc.4980
- Horel, J. D., and J. M. Wallace. 1981. “Planetary-Scale Atmospheric Phenomena Associated with the Southern Oscillation.” Monthly Weather Review 109 (4): 813–29. https://doi.org/10.1175/1520-0493(1981)109<0813:PSAPAW>2.0.CO;2
- Kucharski F, Molteni F, Yoo JH (2006) SST forcing of decadal Indian Monsoon rainfall variability. Geophys Res Lett 33:. https://doi.org/10.1029/2005GL025371
- Kucharski F, Molteni F, King MP, et al (2013) On the need of intermediate complexity general circulation models: A “sPEEDY”’ example.” Bull Am Meteorol Soc 94:25–30. https://doi.org/10.1175/BAMS-D-11-00238.1
- Mezzina, B 2022, Dynamics of the late-winter ENSO teleconnection to the North Atlantic-European region, PhD thesis, University of Barcelona, Barcelona, http://hdl.handle.net/2445/182562
- Smith, Thomas M., Richard W. Reynolds, Thomas C. Peterson, and Jay Lawrimore. 2008. “Improvements to NOAA’s Historical Merged Land-Ocean Surface Temperature Analysis (1880-2006).” Journal of Climate 21 (10): 2283–96. https://doi.org/10.1175/2007JCLI2100.1.
- Straus D, Shukla J, Paolino D, et al (2003) Predictability of the seasonal mean atmospheric circulation during autumn, winter and spring. J Clim.